# Development and evaluation of methotrexate nanocomposites using B-cyclodextrins/alginate polymers and response surface methodology

A. M. Hussein[a], S. H. Hussein-Al-Ali[a,b,*]
[a]*Department of Basic Pharmaceutical Sciences, Faculty of Pharmacy, Isra University, Amman 11622, Jordan*
[b]*Department of Chemistry, Faculty of Science, Isra University, Amman 11622, Jordan*

β-cyclodextrin and alginate polymers have been extensively investigated for their use in drug delivery systems. β-Cyclodextrin-alginate nanoparticles (CD/Alg) as an innovative drug carrier was the preapared by ionic chelation method. Methotrexate (MTX) as model drug was loaded onto the β-CD/Alg nanoparticles to form MTX-CD/Alg nanocomposites, via ionic interactions. The study was to investigate the changes in independent variables (concentration of CD, Alg and $CaCl_2$) loading efficiency and particle size using 4-levels of CD, 5-levels of Alg and 4-levels of $CaCl_2$. The Optimum nanocomposite has %LE (58.1% and particle size (213 nm). The prepared nanocomposites were chrecterized by powder X-ray diffraction (PXRD), Fourier transform infrared spectroscopy (FTIR), a thermogravimetric analysis (TGA) and a release study. FTIR analysis displayed the drug into nanocomposites. The XRD pattern of MTX-β-CD/Ag nanocomposite suggested a peak at 2θ = 44.6° with the amorphous properties. A novel MTX-CD/Alg nanocomposites was developed. Optimized, characterized, and release studied was performed. These nanocomposites will be prmosing by delivering the drug in powder form.

(Received November 1, 2023; Accepted January 30, 2024)

*Keywords:* β-cyclodextrin polymers, Alginate polymers, Nanocomposites, Response surface methodology, Sustained release

## 1. Introduction

Design of experiments (DOE) is a systematic, effective processes that enables researchers to study the relationship between multiple input variables (Independent variables) and key output variables (dependent variables). It is a structured approach for collecting data and applied in industry [1-3]. DOE using to determine whether a factor, factors interact, or a collection of factors, has an effect on the depending on variable (Response). In addition, its used to model the behavior of the response as a function of the factors. Finally, to optimize the response [4-7].

Researchers usually use eight types of DOE, which are as follows: full factorial designs, Fractional factorial designs which called screening designs, response surface designs, mixture designs, Taguchi array designs, split plot designs, definitive screening design, and custom designs [8-11]. Researchers choose one of these types based on the number of factors which need to use, levels of each factor, Possible interaction between factors and Model order [12].

Polymeric nanoparticles (NPs) are tiny particles having size range from 1 to 1000 nm [13], can be used in drug delivery by loaded with active compounds surface-adsorbed onto polymer surface or entrapped within core [14]. In general, the most commonly strategies used for production of polymer nanoparticles are dispersion of preformed polymers and the polymerization of monomers [15, 16]. These strategies lead to form nanospheres polymer nanoparticles through solvent evaporation, emulsification/solvent diffusion, nanoprecipitation, emulsification/reverse salting-out production methods; or forming nanocapsules by nanoprecipitation production methods [17-19].

* Corresponding author: samer.alali@iu.edu.jo
https://doi.org/10.15251/DJNB.2024.191.213

Cyclodextrins are cyclic sugar molecules, composed of glucopyranose units [20]. Three types of cyclodextrins known (α, β and γ) with 6, 7, and 8 glucopyranose units respectively [21]. Recently the cyclodextrins with 3 and 4 glucopyranose units were synthetized [22], and on the other cyclodextrins with more, than 8 glucopyranose units are also known [20]

Cyclodextrins are widely used in pharmaceutical applications, the cyclodextrins research and application is still significant. The main application of cyclodextrins in pharmacy is enhancement of Class 2 and 4 poorly water-soluble drugs and then bioavailability [23]. The structure of it increases the chance for interactions between the cavity and guest drugs [24].

There are many recent studies in which β-cyclodextrin/alginate (β-CD/Alg) nanoparticles have been used to deliver different drugs; for example, the (βCD-Alg) loaded with 5-fluorouracil (5-FU) [25]. The 5FU-βCD-Alg nanocomposite shows effective for 5-FU with strong antiproliferative activity against MCF-7 cells and negligible effects on normal healthy cells [25].

The alginate–chitosan–cyclodextrin micro- and nanoparticulate was loaded with isoniazid and isoconazole as antimycobacterial compounds. The study shows that the It alginate–chitosan–cyclodextrin microparticulate systems loaded with isoniazid and isoconazole are as effective as pure isoniazid applied in higher dosages [26].

Methotrexate is an anti-folate drug which competitively binds with dihydrofolate reductase (DFHR) [27], Primary developed for the treating of malignancies and thereafter utilized in another diseases such as immunosuppressive or anti-inflammatory drug. MTX is now used in the treating of rheumatoid arthritis [28].

Various attempts were carried out to increase the activity of MTX or to decrease their side effect. For example, Lee et al. have prepared methotrexate-poly(lactide-co-glycolide) (PLGA) nanoparticles to Improve Lymphatic Delivery [29]. The methotrexate was loaded on the polymeric lipid hybrid nanoparticles (PLHNPs) for the treatment of glioblastoma [30].

The present paper was aimed at formulating β-Cyclodextrin-alginate nanoparticles containing methotrexate, as a model drug. A full factorial experimental design was applied to study all the possible combinations of the levels of the factors in each complete trial and using response surface regression to identification of the significant main and interaction effects of experimental factors (β-Cyclodextrin, alginate and the $CaCl_2$) in order to find optimal conditions for nanocomposite. In addition, the nanocomposites were characterized in terms of %LE, zeta potential and particle size. Furthermore, in vitro release studies were performed to study the nanocomposites' ability to deliver the methotrexate drug and form sustained release systems.

## 2. Experimental

### 2.1. Materials

The chemicals used in the present study are methotrexate ($C_{20}H_{22}N_8O_5$,>99% purity) was purchased from Sigma-Aldrich (Gillingham, UK), sodium alginate (low viscosity with purity 98%) was purchased from Xilong Chemicals (China), β-cyclodextrin (purity,98%) was purchased from Alfa-Aesar (Germany), Dimethyl Sulfoxide and other chemicals such as sodium hydroxide and calcium chloride was obtained from AZ chemicals (Karachi-Pakistan).

### 2.2. Preparation of β-cyclodextrin/alginate nanoparticles

The solution of β-cyclodextrin polymer was prepared by dissolving different amounts of polymer (50, 100, 200 and 500 mg) into 50 mL of distilled water. In addition, the solution of alginate polymer was prepared by taking different amounts of them (25, 50, 100, 150 and 200 mg) into 50 mL of distilled water. Finally, the solution of $CaCl_2$ was prepared by taking different amounts of them (30, 45, 60 and 75 mg) into 50 mL of distilled water.

Preparation of β-cyclodextrin/alginate nanoparticles was carried out by mixing each selected amount of β-cyclodextrin and alginate, then adding dropwise $CaCl_2$ as crosslinkers. The pH of the component was adjusted at 10 by adding NaOH. The nanoparticles were stirred overnight and then centrifuged at 11,000 rpm. The gel of nanoparticles was washed three times with distilled water and dried in an oven.

### 2.3. Preparation of MTX-CD/Alg nanocomposites

The MTX-CD/Alg nanocomposites were prepared by the following method. The solutions of MTX, β-cyclodextrin and alginate were mixed with each other. The $CaCl_2$ cross-linkers was added to the last mixture solution. The pH was adjusted at 10 by using 0.1 NaOH. MTX-CD/Alg nanocomposites were stirred overnight and then centrifuged at a speed of 11,000 rpm for 20 min. The MTX-CD/Alg nanocomposites were washed three times with distilled water and dried in an oven.

### 2.4. Determination of Loading Efficiency (%LE) of MTX

The ultra-centrifugation instrument was used to separate the supernatant from the prepared nanocomposites. The concentration MTX drug in the supernatant was calculated from the absorbance at a $\lambda_{max}$ of 370 nm measured by ultraviolet–visible spectrophotometer. The % LE of MTX was calculated with Equation 1.

$$\%\text{Loading} = \frac{\text{Total mass of MTX} - \text{Total mass of free MTX}}{\text{mass of nanocomposites}} \times 100 \quad (1)$$

### 2.5. Particle size analysis

Particle size of MTX-CD/Alg nanocomposites was determined by using dynamic light scattering. The samples were dispersed in distilled water and sonication for 15 minutes. Fill the cuvette and cap the cuvette. Malvern logo should be oriented towards the front of the instrument and checking there are no bubbles in the cuvette.

### 2.6. In vitro release study of methotrexate from MTX-CD/Alg nanocomposites

In vitro release of methotrexate from nanocomposites was determined in PBS at pH 7.4, using a Perkin Elmer UV-vis spectrophotometer with $\lambda_{max}$ of 370 nm. A suitable amount of each nanocomposite was added to the release media. The cumulative amount of methotrexate released into the solution was measured every 10 minutes by kinetic studying UV-vis spectrophotometer for 24 hours at corresponding $\lambda_{max.}$ The percentage release of methotrexate in the PBS was obtained in equation 2

$$\%\text{Release} = \frac{\text{Concentration of MTX at time t (ppm)}}{\text{Concentration of MTX in nanocomposite (ppm)}} \times 100 \quad (2)$$

### 2.7. Full Factorial Design (FFD) for Design of experiments

During the MTX-CD/Alg nanocomposites development, Full Factorial Design was used which discrete possible levels, and take all possible combinations of these levels across all such factors. Four levels for β-cyclodextrin and $CaCl_2$, and five levels for sodium alginate was used in this work (Table 1). According to the applied design, a total of 36 experimental runs were generated and randomly performed. As the response variables, % LE, particle size, and zeta potential were determined.

*Table 1. Levels for β-CD, Alg and $CaCl_2$.*

| **Parameters (mg)** | **Levels** | | | | |
|---|---|---|---|---|---|
| | **1** | **2** | **3** | **4** | **5** |
| **β-CD** | 50 | 100 | 200 | 500 | * |
| **Alg** | 25 | 50 | 100 | 150 | 200 |
| **$CaCl_2$** | 30 | 45 | 60 | 75 | * |

### 2.7. Instrumentation

X-ray diffraction (XRD) is a technique used widely to identify the structure of crystalline materials. The range at 2-70 degrees using CuK radiation (λ 1.54.6 Å) at 30 kV and 30 mA. Fourier transform infrared spectroscopy (FTIR) is a technique used for identifying functional groups and chemical bonds that are present in a molecule, interpreted from the observed infrared absorption spectrum. FTIR spectra of the materials were recorded over the range of 400-4000$cm^{-1}$ on a Perkin Elmer (model smart UAIR-tow) with 4 $cm^{-1}$ resolutions. Particle size of MTX-CD/Alg nanocomposites was determined by using dynamic light scattering (DLS) with Zetasizer (Malvern, UK). Ultraviolet–visible spectrophotometry (UV-Vis) was used to quantitatively measure the drug release, a Shimadzu UV-1601 spectrophotometer. Thermogravimetric and differential thermogravimetric analyses were carried out using a Mettler Toledo instrument with a heating rate of 10°C per minute in the range of 20-1000°C under a nitrogen atmosphere (nitrogen flow rate 50 mL per minute).

## 3. Results and discussion

### 3.1. ANOVA values for loading efficiency and particle size

Analysis of variance that related to %LE and particle size is shown in Table 2. By using P-value and F-value it was explained that the models used in analysis (linear, square and 2-way interaction) are statistically significant, because their P-values are lower than 0.05 and F-values are high. On another hand, when the result explained deeply, several variables hadn't been significant effect on LE such as β-CD, $CaCl_2$, β-CD*β-CD and $CaCl_2$* $CaCl_2$.

Table 2, represents the significant and non-significant variables affecting particle size. Alg, β-CD, Alg*Alg and $CaCL_2$*$CaCl_2$ are significantly affecting particle size because the p-value is lower than 0.05 and high F-values. On the other hand, the particle size is non-significant at significant level of 0.05 affecting by other variables such as $CaCl_2$, β-CD*β-CD and totally 2-way interaction.

*Table 2. ANOVA values for %LE and particle size.*

| **LE model** | | | | | | | | |
|---|---|---|---|---|---|---|---|---|
| | DF | Adj SS | Adj MS | F value | Coef | T Value | VIF | P value |
| **Model** | 9 | 12112.6 | 1345.84 | 68.81 | 16.92 | 10.79 | - | 0.000 |
| **Linear** | 3 | 10053.7 | 3351.22 | 171.33 | - | - | - | 0.000 |
| Alg | 1 | 9964.7 | 9964.73 | 509.45 | -18.487 | -22.57 | 1.10 | 0.000 |
| B-CD | 1 | 12.3 | 12.33 | 0.63 | -0.562 | -0.79 | 1.08 | 0.431 |
| $CaCl_2$ | 1 | 7.4 | 7.36 | 0.38 | -0.492 | -0.61 | 1.11 | 0.542 |
| **Square** | 3 | 2940.2 | 980.06 | 50.11 | - | - | - | 0.000 |
| Alg*Alg | 1 | 2929.4 | 2929.4 | 149.77 | 16.87 | 12.24 | 1.04 | 0.000 |
| B-CD*B-CD | 1 | 17.9 | 17.89 | 0.91 | -1.56 | -0.96 | 1.11 | 0.343 |
| $CaCl_2$*$CaCl_2$ | 1 | 10.7 | 10.71 | 0.55 | 0.93 | 0.74 | 1.04 | 0.462 |
| **2-Way Interaction** | 3 | 341.8 | 113.94 | 5.83 | | - | - | 0.002 |
| Alg*B-CD | 1 | 96.0 | 96.03 | 4.91 | -2.144 | -2.22 | 1.10 | 0.031 |
| Alg*$CaCl_2$ | 1 | 157.7 | 157.7 | 8.06 | -3.19 | -2.84 | 1.06 | 0.006 |
| B-CD*$CaCl_2$ | 1 | 107.5 | 107.5 | 5.50 | 2.162 | 2.34 | 1.10 | 0.023 |
| **Size model** | | | | | | | | |

| LE model | | | | | | | | |
|---|---|---|---|---|---|---|---|---|
| | DF | Adj SS | Adj MS | F value | Coef | T Value | VIF | P value |
| **Model** | 9 | 73235.2 | 8137.2 | 13.72 | 221.2 | 20.94 | - | 0.000 |
| **Linear** | 3 | 39565.1 | 13188.4 | 22.24 | - | - | - | 0.000 |
| Alg | 1 | 27872.1 | 27872.1 | 47.00 | -32.75 | -6.86 | 1.16 | 0.000 |
| B-CD | 1 | 15836.4 | 15836.4 | 26.70 | -24.05 | -5.17 | 1.20 | 0.000 |
| $CaCl_2$ | 1 | 2144.7 | 2144.7 | 3.62 | -9.66 | -1.90 | 1.18 | 0.064 |
| **Square** | 3 | 13061.2 | 4353.7 | 7.34 | - | - | - | 0.000 |
| Alg*Alg | 1 | 6194.3 | 6194.3 | 10.45 | 27.45 | 3.23 | 1.03 | 0.002 |
| B-CD*B-CD | 1 | 82.2 | 82.2 | 0.14 | -3.9 | -0.37 | 1.18 | 0.712 |
| $CaCl_2$*$CaCl_2$ | 1 | 7195.5 | 7195.5 | 12.13 | -28.09 | -3.48 | 1.12 | 0.001 |
| **2-Way Interaction** | 3 | 1729.6 | 576.5 | 0.97 | | - | - | 0.415 |
| Alg*B-CD | 1 | 1253.4 | 1253.4 | 2.11 | 9.02 | 1.45 | 1.25 | 0.153 |
| Alg*$CaCl_2$ | 1 | 2.6 | 2.6 | 0.00 | 0.43 | 0.07 | 1.15 | 0.948 |
| B-CD*$CaCl_2$ | 1 | 674.0 | 674.0 | 1.14 | 6.93 | 1.07 | 1.28 | 0.292 |

The response surface design and the responses of LE and particle size are shown in equations 3 and 4. To fit the experimental data, a full quadratic model was applied.

**LE**=66.37 - 0.5920 Alg + 0.0043 β-CD - 0.150 $CaCl_2$ + 0.002204 Alg*Alg - 0.000031β-CD*β-CD + 0.00184 CaCl2*$CaCl_2$ - 0.000109 Alg*β-CD - 0.001622 Alg*$CaCl_2$ + 0.000427 β-CD*$CaCl_2$ (3)

**Size**= 237.0 – 1.318 Alg – 0.188 β-CD + 5.00 $CaCl_2$ + 0.00358 Alg*Alg – 0.000077 β-CD*β-CD – 0.0555 CaCL2*$CaCl_2$ + 0.000458 Alg*β-CD + 0.00022 Alg*$CaCl_2$ + 0.00137 β-CD*$CaCl_2$ (4)

### 3.2. Residual plots for loading efficiency, and particle size

High value of $R^2$ and approximate straight line of Normal Probability plot as was shown in Figure 1 that can support the model which was chosen to be studying the effect of variables on loading efficiency and particle size. In addition, the result of $R^2$ values for loading efficiency and particle size have value of 91.84% and 74.62% respectively, related to linearity of normal probability plot.

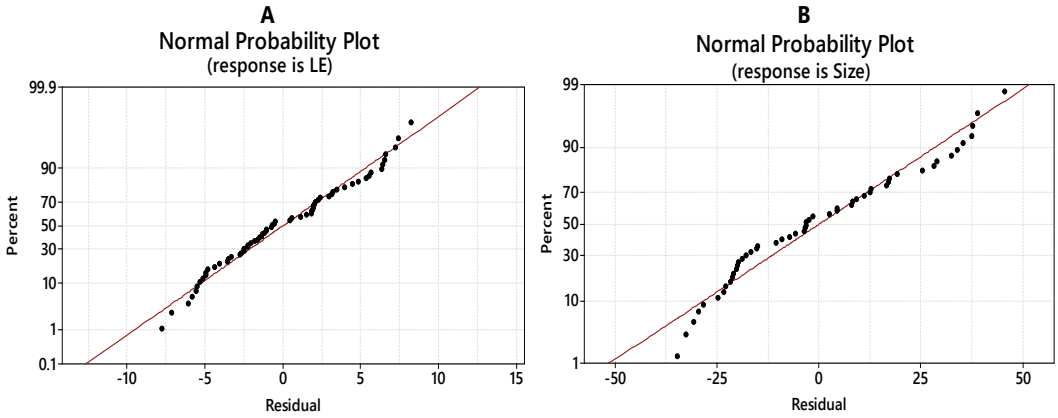


*Fig. 1. Normal probability plot of residuals.*

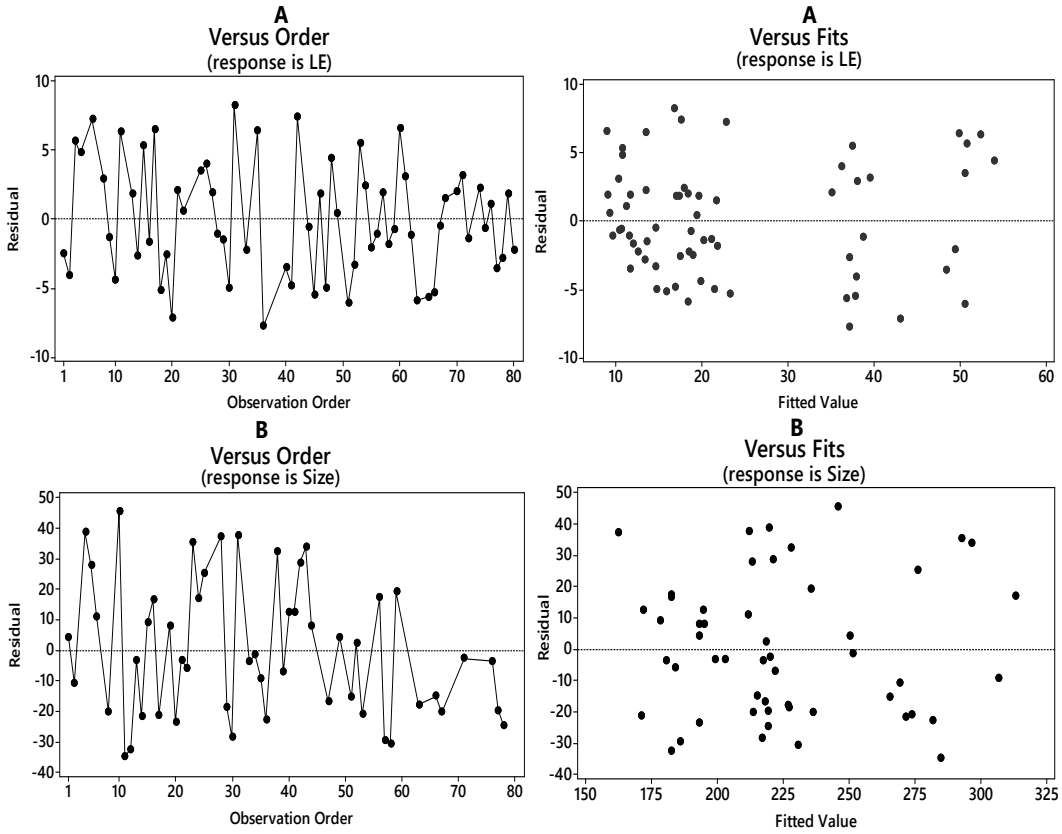


*Fig. 2. Residual versus order and fits of data.*

Based on **Figure 2** that are explained the residuals versus order plot and residuals versus fits plot for loading efficiency and particle size, which indicates that the plots do not follow any systematic pattern. Thus, the model did not contain any probability of systematic errors.

### 3.3. Pareto charts of the standardized effects for loading efficiency, and particle size

The Pareto chart displays the standardized effects absolute value from the biggest impact to the smallest impact. A reference line also is plotting on the Pareto chart to suggest which impacts are statistically important (significant). The effectiveness of dependent and independent variables on loading efficiency are shown in Figure 3A by using Pareto chart, which explained that bars of alginate, alginate*alginate and their interactions with other variables passed the reference line that is at 2.00. This means these factors are significantly affecting loading efficiency at the 0.05 level. Also, this plot clearly explained that the alginate and alginate*alginate are mostly significant affecting on loading efficiency than other variables. On the Pareto chart, which is represented on Figure 3B of particle size, bars of alginate, β-CD, $CaCl_2$*$CaCl_2$ and alginate*alginate which are crossed the reference line that is at 2.018. This means these factors are mostly significant affecting on particle size at the 0.05 level.

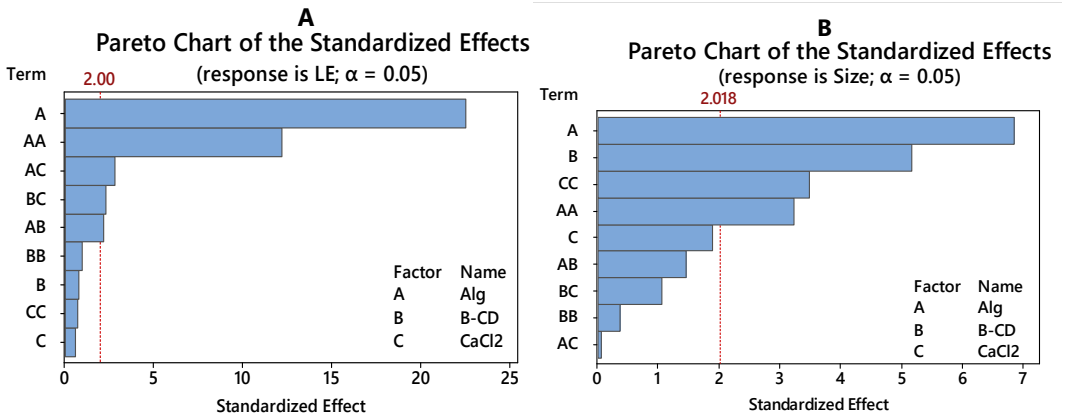


*Fig. 3. Pareto charts of the standardized effects on loading efficiency (A) and particle size (B).*

### 3.4. Main effect plots for loading efficiency and particle size

Main effects plot can explain the effect of each variable on different levels, which are connected to each other by line on outcome or response. Figure 4A shows the results by using plot called main effects plot, which suggested that alginate, β-CD and $CaCl_2$ were factors that had an effect to loading efficiency. By increasing concentration of alginate, the loading efficiency tended to decrease until the concentration of alginate reached 150 mg then when alginate concentration is increased greater than 150 the loading efficiency is increased. On the other hand, an increase or decrease in β-cyclodextrin or $CaCl_2$ concentration would not affect significantly on loading efficiency.

Depending on the Figure 4A, loading efficiency values are decreased with increasing of sodium alginate concentration may be due to the possibility of increasing the binding of beta cyclodextrin and alginate and decreasing the probability of ionic bond between MTX and polymers.

Main effects plot particle size is shown in Figure 4B, which indicates and supports the information mentioned in Figure 3B of contour plots. Main effects represented the effecting of alginate on particle size by inverse relationship until 150 mg of alginate, then if alginate is used in amount greater than 150 mg, the relationship between alginate and particle size is proportional. Although $CaCl_2$ affects the size of particles in a direct way until the concentration of $CaCl_2$ reaches 50 mg, after which the effect becomes reverse, while the use of β-CD always adversely affects the particle size.

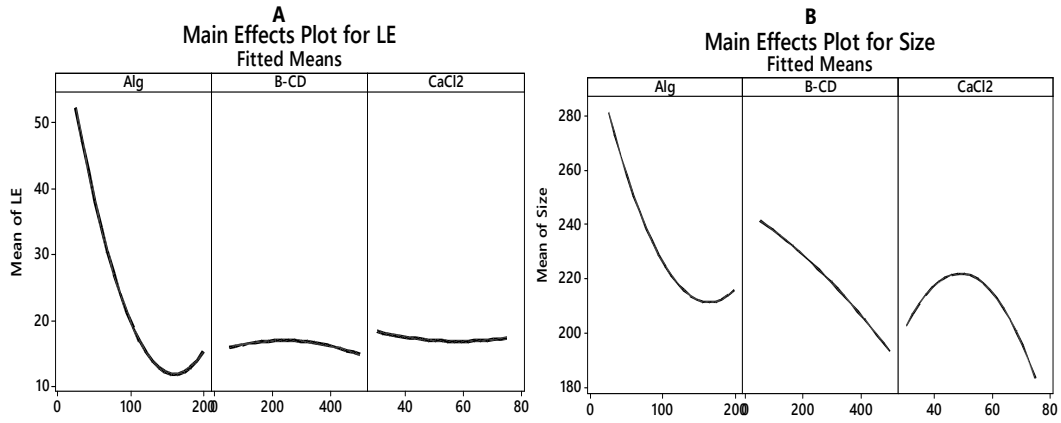


*Fig. 4. Main effects plot for loading efficiency (A) and particle size (B).*

### 3.5. Interaction plots for loading efficiency and particle size

Interaction plot is used to represent how the value of one parameter effect on relationship between another parameter and a response. This plot shows on x-axis the different levels of one factor and a detail line of another factor for different levels. If the lines are parallel then, no interaction between variables, but if the lines are not parallel,

Significant interaction is shown between variables. Figure 5A represents the interaction between alginate with each of $CaCl_2$ and β-CD depending on the different values of $CaCl_2$ and β-CD. Therefore, the lines are not parallel, that indicates significant interaction between the alginate with β-CD and $CaCl_2$. Also, a significant interaction between β-CD and $CaCl_2$ appears in Figure 5A.

To explain significant interactions between the method factors, interaction plots of average size of particles for the factor in each level with the constant level of another factor are represented in Figure 5B. It represented no interaction between calcium chloride and alginate; this is because the levels lines are parallel. Although the plot lines of Alg * β-CD and β-CD *CaCl2 don't cross each other, it shows significant interaction this is because the lines absence of parallelism.

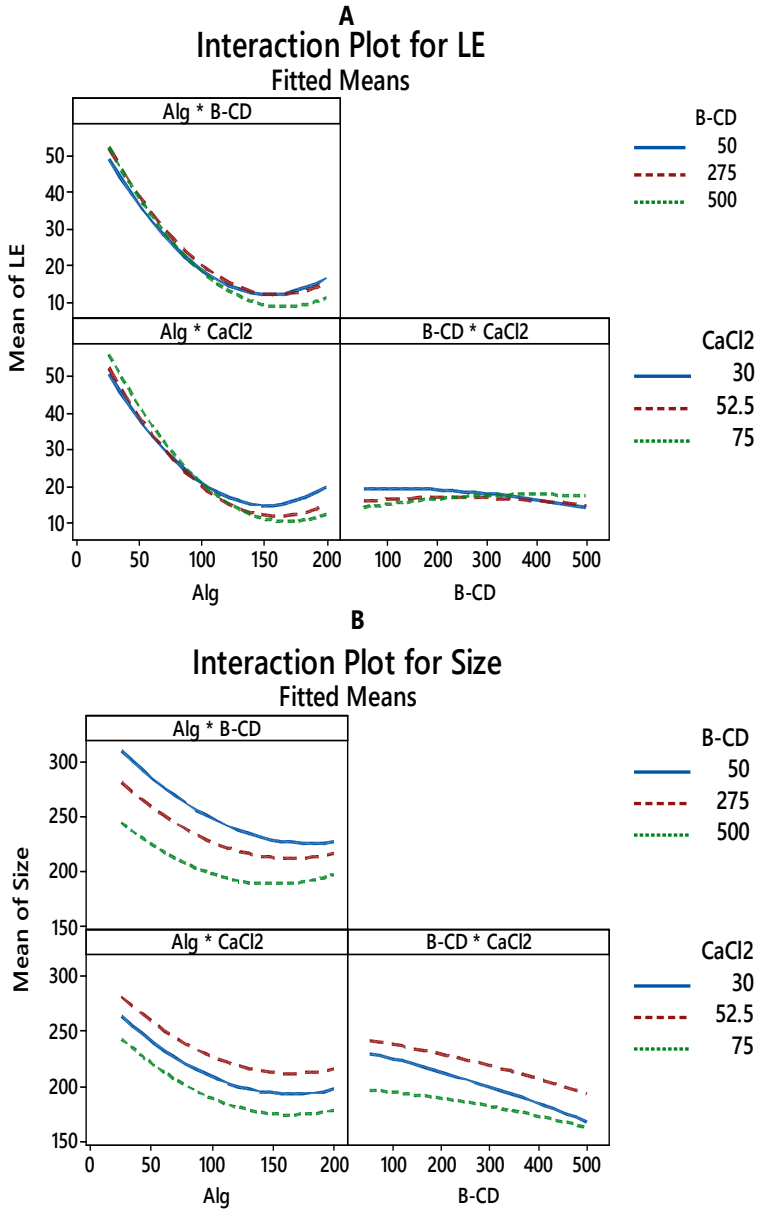


*Fig. 5. Interaction plot for loading efficiency (A) and particle size (B).*

### 3.6. Optimization of the models

**Figure 6** shows an optimized concentration for the response factors loading efficiency and particle size. The optimized formula selected had the highest %LE with value 58.1% and the smallest particle size with value 213 nm.

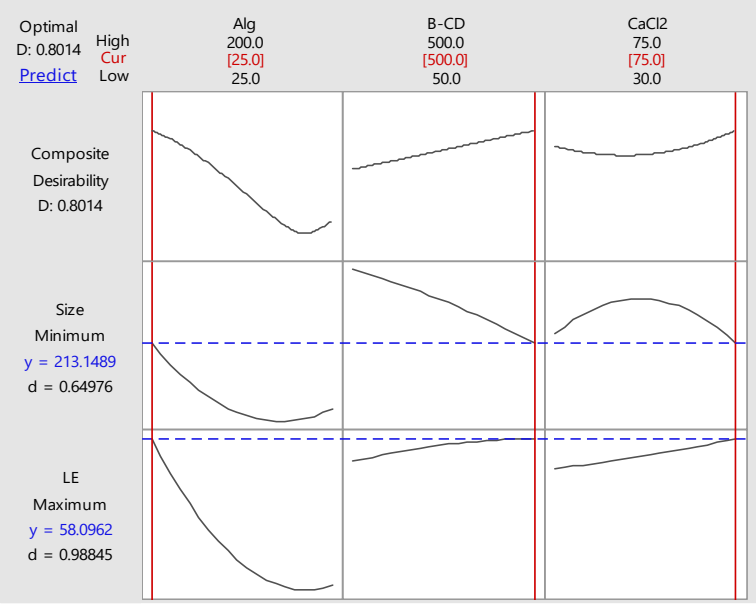


*Fig. 6. The optimized concentrations for loading efficiency and particle size.*

### 3.7. Validation of the models

A bias formula under optimized factors was performed to compare with the predicted values. As shown in **Table 3**, the bias was around -5.0%, and -4.3% for first formula (β-CD= 500 mg, Alg=41 mg and $CaCl_2$= 30 mg). In addition, the bias was around -7.5% and -4.4 for second formula (β-CD= 303mg, Alg= 25 mg and $CaCl_2$= 71 mg) and around -8.7%, and -5.0% for third formula (β-CD= 494mg, Alg= 90mg and $CaCl_2$= 71 mg), respectively. These results indicate the validity of generated models with no statistically significant difference and good correlation between predicted and experimental values.

*Table 3. Comparison of the observed and predicted value of the response variables of optimized formulation.*

| concentrations | Experimental Response | Predicted values | Observed values | Bias (%) |
|---|---|---|---|---|
| β-CD 500 mg Alg 41 mg $CaCl_2$ 30 mg | LE (%) | 39.5% | 38% | -5.0% |
| | Particle size (nm) | 206 nm | 197 nm | -4.3% |
| β-CD= 303 mg Alg= 25 mg $CaCl_2$= 71mg | LE (%) | 55.6% | 51.4% | -7.5% |
| | Particle size (nm) | 250 nm | 239 nm | -4.4% |
| β-CD= 494 mg Alg= 90 mg $CaCl_2$= 71mg | LE (%) | 24% | 21.9% | -8.7% |
| | Particle size (nm) | 180 nm | 171 nm | -5.0% |
| **Bias was calculated as (observed value-predicted value/predicted value)×100%** | | | | |

### 3.8. Characterization of MTX-CD/Alg nanocomposites

#### *3.8.1. X-ray diffraction (XRD)*

The XRD was used to clarify polymorphism and molecular structure of polymeric nanocomposites. Figure 7 A, B and C represent the XRD patterns of methotrexate, β-cyclodextrin and methotrexate loaded β-CD/Alg nanocomposites, respectively.

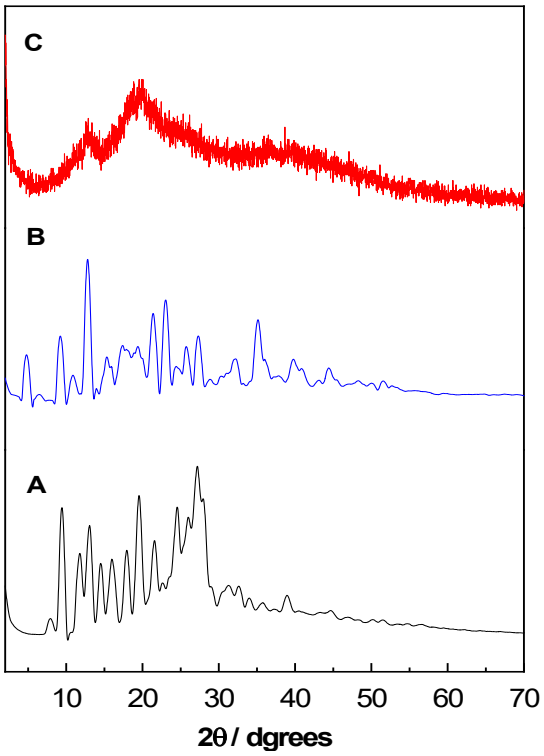


*Fig. 7. X-Ray diffraction of MTX (A), β- CD (B) and MTX-CD/Alg nanocomposites (C).*

At Figure 7A, free methotrexate XRD pattern from 2-70° has a polycrystalline peak at 13.7, 14.1, 19.6, 27.8 and 29 degrees with strongly absorption which that obtained comparable crystalline methotrexate XRD pattern was reported in literature [31]. Figure 7B shows the β-CD XRD pattern evidences a clarify crystalline nature because it have a sharp and intense peaks at 4.5, 8 and 15 degrees, in addition when compared these peaks with pattern of inclusion complexes, peaks at 4.5 and 8 disappeared [32]. On another hand, when the free methotrexate compared with MTX-β-CD/Alg nanocomposites pattern as shown in Figure 7C which that displayed lines devoid any sharpness peaks. This result could be clarified by the strong interaction which destroyed the close packing for beta cyclodextrin substances for the formation of crystallites between methotrexate and beta cyclodextrin.

#### *3.8.2. Fourier transform infrared (FT-IR)*

To characterize the interactions in the MTX-CD/Alg nanocomposites, spectra of FT-IR were analysed. FT-IR spectra of MTX, β-CD, β-CD/Alg and MTX-β-CD/Alg nanocomposites are shown in Figure 8.

The peaks as broad band of MTX at Figure 8A that appeared in 3450 $cm^{-1}$ and 3080 $cm^{-1}$ that assigned to hydroxyl group (OH) from carboxyl group and primary amine stretching respectively. But the bands of N-H bending from group of amide appeare in the (1550-1500) $cm^{-1}$ range and overlapping with the -C=C stretching aromatic group. Another bands from carboxylic acid corespond to C-Ostretching at (1400-1200) $cm^{-1}$ spectral range. At (1600-1670) $cm^{-1}$ indicate to (C=O) stretching from carboxylic acid [33].

The FT-IR spectrum of β-CD in Figure 8B was showed a stretching peak at (3300-33400) $cm^{-1}$ spectral range duo to the hydroxyl group (OH). Also peaks at1029 and 1153 $cm^{-1}$ indicated C-H, C-O stretching. In addition 1153 $cm^{-1}$ peak that inducated the absorption of the C-O-C vibration [34]. After the reaction between calcium alginate and beta cyclodextrin was obtained and was shown at Figure 8C, the broad band at 3340 $cm^{-1}$ of beta cyclodextrin shifts to 3430 $cm^{-1}$ and the peaks at 1157 shifted by a few $cm^{-1}$ [35]. In Figure 4.16 C, the the broad band at 3430 $cm^{-1}$ is indicated to the O-H vibration which that wide and range, because alginate and β-CD have a O-H group in their structure.

Spectrum of MTX-β-CD/Alg nanocomposites is compared with the spectrum of the β-CD/Alg as blank in Figure 8D, two specific peakes of methotrexate appeared at 3450 $cm^{-1}$ and 3080 $cm^{-1}$, signalizing incorporating of methotrexate into methotrexate loadded β-CD/Alg nanocompositeswith minor shifting.

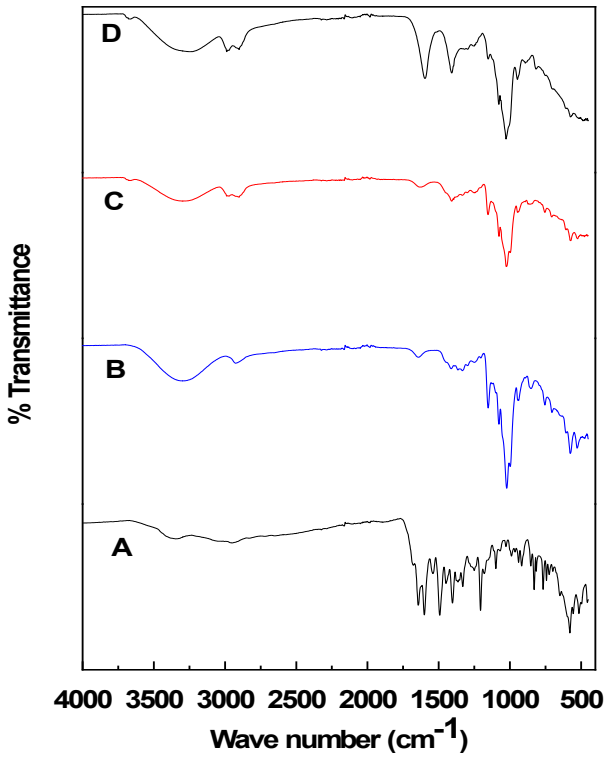


*Fig. 8. FTIR spectrum of MTX (A), β- CD (B), Alg-βCD (C) and MTX-Alg-βCD nanocomposites (D).*

### *3.8.3. Interaction between the components of the nanocomposites*

Possible interaction between the MTX, CD and Alg polymers is shown in Figure 9. From the Figure, it can be seen that β-CD and Alg chains polymers electrostatically interact between negative charge of β-CD and Alg polymers and positive charge of $CaCl_2$. Based on the structure of MTX that contains carboxyl (COOH-) and amine ($NH_2$) groups, MTX results to formation of several hydrogen bonds with β-CD and Alg polymers as shown in Figure 9.

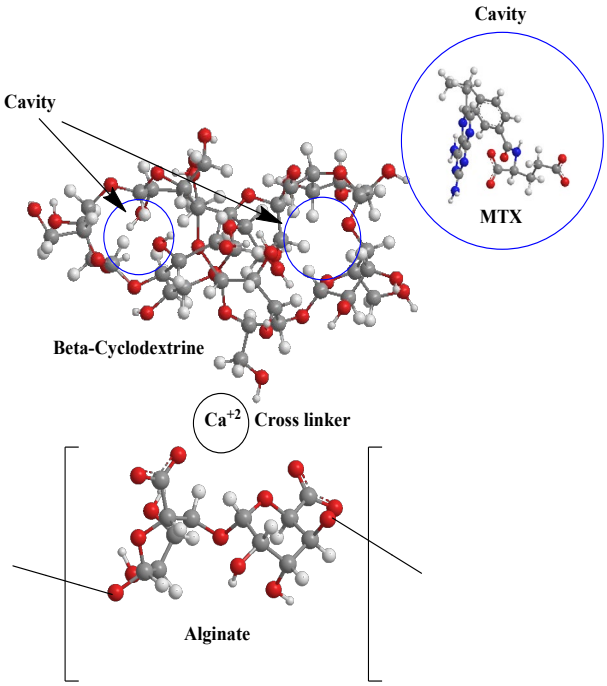


*Fig. 9. Possible interaction between the components of MTX-CD-Alg nanocomposites.*

### *3.8.4. Thermogravimetric Analysis (TGA)*

The thermogravimetric and differential thermogravimetric analyses obtained for MTX, β-CD, CD-Alg nanoparticles and MTX-CD-Alg nanocomposites are shown in Figure 10. As shown in Figure 10A, initially 9% of the weight was lost up to 192 °C, followed by a rapid decomposition at 350 °C, resulting in approximately 38% weight loss [36, 37]. Figure 10B shows thermogravimetric analyses of β-CD. the loses water in the 50-192 ºC interval and starts degradation at about 277 ºC [38, 39]. Figure 10C shows four weight losses for MTX- βCD-Alg nanocomposites with temperature maxima at 113°C, 243°C, 318°C, and 458°C, corresponding to weight losses of 16.0%, 32.4%, 8.9%, and 8.4%, respectively. The first mass loss was due to the removal of water molecules. The second, third and fourth mass losses in the range of 205°C–598°C were due to decomposition of CD and MTX. Increasing the decomposition rate of nanocomposites comparing with CD and MTX indicates the greater thermal stability of MTX in MTX- βCD-Alg nanocomposites.

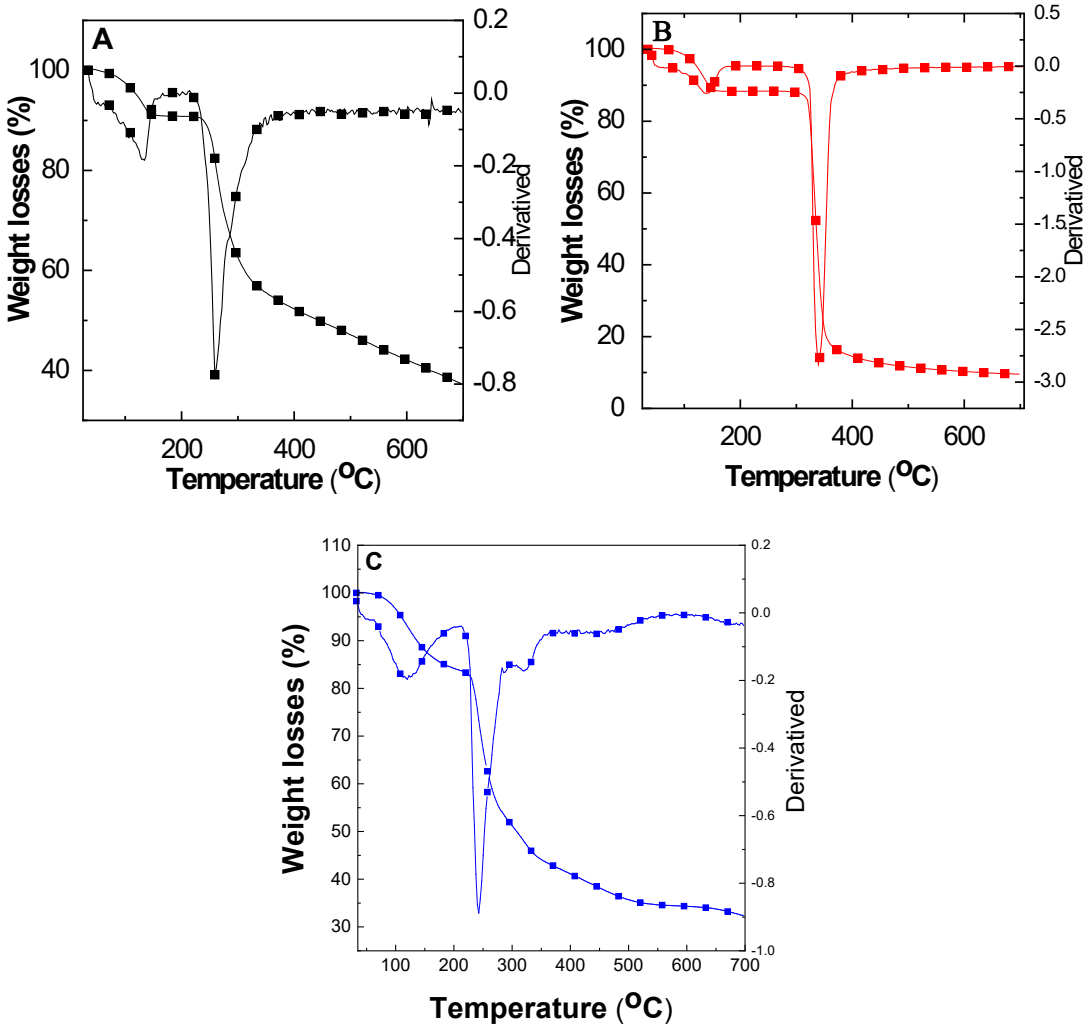


*Fig. 10. Thermogravimetric analysis of MTX (A), β-CD (B), and MTX-CD-Alg nanocomposites (C).*

### *3.8.5. In Vitro release study*

Release curves of methotrexate from MTX-β-CD-Alg nanocomposites at pH 7.4 as a function of time are shown in Figure 11. It can be noticed that MTX released was approximately 60 % after 24 hours. This release may have been covered by several mechanisms. Swelling of hydrogel beads is one of the main mechanism play an important role in drug release by intake of water to enter through polymer unto dissolving of polymer (alginate) [40]. Also, diffusion and erosion were possible mechanisms of MTX release from matrix of polymer containing cyclodextrin, by diffusion process the drug penetrate during the inside of the matrix of polymer to the surrounding area while erosion process which polymer degradation may lead bonds break [41]. The degradation process depending on several factors can be affects on degradation such as: enzymes on the surrounding media, pH value of surrounding medium, composition with another polymer and uptake of water via the polymer [42-44].

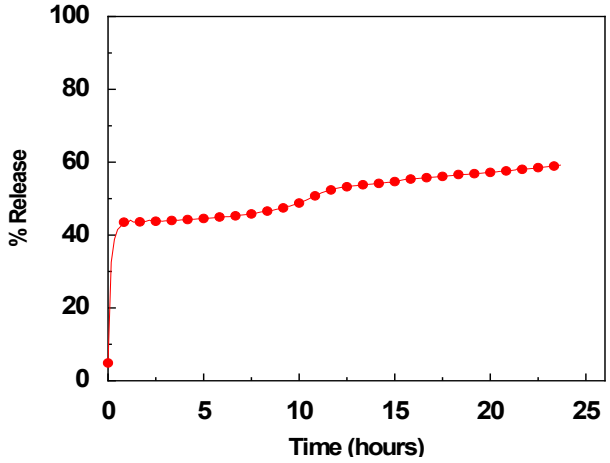


*Fig. 11. In vitro release of MTX from MTX-β-CD-Alg nanocomposites in the pH 7.4.*

### *3.8.6. Release kinetics of MTX from the β-CD/Alg nanocomposites*

Five kinetics models which that generally described the data of the MTX cumulative release from nanocomposites as follows (Table 4) [45].

| kinetic model | Equations | Terms |
|---|---|---|
| First order | $\ln (q_e-q_t) = \ln q_e - k_1 t$ | $\mathbf{k_1}$ is the first order rate constant.<br>$\mathbf{q_t}$ quantity released at any time.<br>$\mathbf{q_e}$ quantity released at equilibrium. |
| Second order | $t/q_t = 1/k\ q\ 2 + t/q$ | $\mathbf{k_2}$ is the second order rate constant |
| Higuchi model | $qt = KH \times t1/2$ | $k_H$ is the Higuchi rate constant |
| Hixson-Crowell model | $(M_o)^{1/3} – (q_t)^{1/3} = Kt$ | $\mathbf{M_o}$ is the initial quantity of drug |
| Korsmeyer-Peppas model | $q_t/q_\infty = Kt^n$ | $q_\infty$ is the release of drug from nanocomposites at infinite time. |

The MTX release from nanocomposites was described by first order kinetics model, second order kinetics model, Higuchi model, Hixson Crowell model and Korsmeyer Peppas model. By applying these models, the nanocomposite was fitted by second order kinetics model by $R^2$ value 0.992.

## 4. Conclusion

In this study the main aim was obtained to understanding the suitable conditions to estimate the optimized formulations of β-cyclodextrin/Alginate nanocomposites as carrier for hydrophobic drugs and to evaluate the factors which affecting on the loading efficiency, and particle size by using minitab 18.1 software.The results indicated that the alginate is the most factor can play an important role to effecting on LE%, and particle size. Also, the synthesized carrier of β-CD/Alg nanocomposites could overcome the hydrophobicity of some drugs such as methotrexate wich was used as a model drug in this study and increased the loading to reach between 58.1 % in some conditions with an average particle size of 235 nm. In addition, FTIR test was done to estimate the functional groups of components of MTX-β-CD/Alg nanocomposites and XRD test to clarify the interaction between MTX and the blank. Moreover, in vitro release for MTX was presented a prolonged release from MTX-β-CD/Alg nanocomposites.

**Acknowledgements**

The author would like to thank the Faculty of Pharmacy at Isra University for providing funding for this research under grand number 2020/2021/6-23.

## References

[1] Decaestecker, T.N., et al., Journal of Chromatography A, 2004. 1056(1-2): p. 57-65; https://doi.org/10.1016/j.chroma.2004.06.010

[2] Gümüş, D. and F. Gümüş, Arabian journal for science and engineering, 2022. 47(6): p. 7325-7334; https://doi.org/10.1007/s13369-021-06235-w

[3] Ivanova, V. and A. Trendafilova, Macedonian Journal of Chemistry and Chemical Engineering, 2022. 41(1): p. 111-117; https://doi.org/10.20450/mjcce.2022.2483

[4] Liu, W.-Y., et al., Molecules, 2021. 26(10): p. 3031; https://doi.org/10.3390/molecules26103031

[5] Lincha, V.R., et al., International journal of pharmaceutics, 2021. 601: p. 120523; https://doi.org/10.1016/j.ijpharm.2021.120523

[6] Upadhya, R., et al., Advanced Drug Delivery Reviews, 2021. 171: p. 1-28; https://doi.org/10.1016/j.addr.2020.11.009

[7] Aldawood, F., S. Desai, A. Andar. Proceedings of the 2021 IISE Annual Conference. 2021.

[8] Minocha, N., S. Saini, and P. Pandey, TMR Pharmacol Res, 2022. 2(3): p. 10; https://doi.org/10.53388/PR202202010

[9] Diniz, C.A., et al., Applied Composite Materials, 2022: p. 1-30; https://doi.org/10.1007/s10443-022-10046-z

[10] Phanphet, S., et al., International Journal of Global Optimization and Its Application, 2022. 1(1): p. 32-38; https://doi.org/10.56225/ijgoia.v1i1.11

[11] Melero, M., et al., Journal of Sound and Vibration, 2022: p. 117229; https://doi.org/10.1016/j.jsv.2022.117229

[12] Khanam, N., et al., Int J App Pharm, 2018. 10(2): p. 7-12; https://doi.org/10.22159/ijap.2018v10i2.24482

[13] Zielińska, A., et al., Molecules, 2020. 25(16): p. 3731; https://doi.org/10.3390/molecules25163731

[14] Liechty, W.B., et al., Annual review of chemical and biomolecular engineering, 2010. 1: p. 149; https://doi.org/10.1146/annurev-chembioeng-073009-100847

[15] Reis, C.P., et al., Nanomedicine: Nanotechnology, Biology and Medicine, 2006. 2(1): p. 8-21; https://doi.org/10.1016/j.nano.2005.12.003

[16] Amgoth, C., et al., 2019, IntechOpen; https://doi.org/10.5772/intechopen.84424

[17] Bennet, D., S. Kim, Polymer nanoparticles for smart drug delivery. Vol. 8. 2014: chapter; https://doi.org/10.5772/58422

[18] Hernández-Giottonini, K.Y., et al., RSC advances, 2020. 10(8): p. 4218-4231; https://doi.org/10.1039/C9RA10857B

[19] Kovachovska, E.T., et al., Macedonian Journal of Chemistry and Chemical Engineering, 2022. 41(1): p. 65-76; https://doi.org/10.20450/mjcce.2022.2478

[20] Szejtli, J., Chemical reviews, 1998. 98(5): p. 1743-1754; https://doi.org/10.1021/cr970022c

[21] Haimhoffer, Á., et al., Scientia Pharmaceutica, 2019. 87(4): p. 33; https://doi.org/10.3390/scipharm87040033

[22] Ikuta, D., et al., Science, 2019. 364(6441): p. 674-677; https://doi.org/10.1126/science.aaw3053

[23] Loftsson, T., Journal of inclusion phenomena and macrocyclic chemistry, 2002. 44(1): p. 63-67; https://doi.org/10.1023/A:1023088423667

[24] Morin-Crini, N., et al., Progress in Polymer Science, 2018. 78: p. 1-23; https://doi.org/10.1016/j.progpolymsci.2017.07.004
[25] Nguyen, C.-H., et al., Arabian Journal of Chemistry, 2022. 15(6): p. 103814; https://doi.org/10.1016/j.arabjc.2022.103814
[26] Ivancic, A., et al., Beilstein journal of nanotechnology, 2016. 7(1): p. 1208-1218; https://doi.org/10.3762/bjnano.7.112
[27] Genestier, L., et al., Immunopharmacology, 2000. 47(2-3): p. 247; https://doi.org/10.1016/S0162-3109(00)00189-2
[28] Williams, H.J., et al., Arthritis & Rheumatism: Official Journal of the American College of Rheumatology, 1985. 28(7): p. 721-730; https://doi.org/10.1002/art.1780280702
[29] Jang, J.-H., S.-H. Jeong, Y.-B. Lee, International journal of molecular sciences, 2019. 20(13): p. 3312; https://doi.org/10.3390/ijms20133312
[30] Bhattacharya, S., Journal of Experimental Nanoscience, 2021. 16(1): p. 344-367; https://doi.org/10.1080/17458080.2021.1983172
[31] Kumari, S.D.C., et al., Indian Journal of Research in Pharmacy and Biotechnology, 2013. 1(6): p. 915.
[32] Abarca, R.L., et al., Food chemistry, 2016. 196: p. 968-975; https://doi.org/10.1016/j.foodchem.2015.10.023
[33] Fuliaş, A., et al., Digest Journal of Nanomaterials and Biostructures, 2014. 9(1): p. 93-98.
[34] Rachmawati, H., C.A. Edityaningrum, R. Mauludin, Aaps Pharmscitech, 2013. 14(4): p. 1303-1312; https://doi.org/10.1208/s12249-013-0023-5
[35] Nguyen, T.-D., et al., Chemical and biochemical engineering quarterly, 2015. 29(3): p. 429-435; https://doi.org/10.15255/CABEQ.2014.2092
[36] Kondiah, P.P., et al., Biomedicines, 2022. 10(7): p. 1470; https://doi.org/10.3390/biomedicines10071470
[37] Bajas, D., et al., Polymers, 2021. 13(1): p. 161; https://doi.org/10.3390/polym13010161
[38] Marangoci, N., et al., Results in pharma sciences, 2011. 1(1): p. 27-37; https://doi.org/10.1016/j.rinphs.2011.07.001
[39] Sambasevam, K.P., et al., International journal of molecular sciences, 2013. 14(2): p. 3671-3682; https://doi.org/10.3390/ijms14023671
[40] Mahdavinia, G.R., et al., Journal of Biomaterials Science, Polymer Edition, 2014. 25(17): p. 1891-1906; https://doi.org/10.1080/09205063.2014.956166
[41] Bibby, D.C., N.M. Davies, I.G. Tucker, International journal of pharmaceutics, 2000. 197(1-2): p. 1-11; https://doi.org/10.1016/S0378-5173(00)00335-5
[42] Fonseca-Santos, B. and M. Chorilli, Materials Science and Engineering: C, 2017. 77: p. 1349-1362; https://doi.org/10.1016/j.msec.2017.03.198
[43] Sabbagh, H.A.K., et al., Journal of Polymer Research, 2019. 26(8): p. 1-14; https://doi.org/10.1007/s10965-019-1854-x
[44] Yang, M., et al., Digest Journal of Nanomaterials and Biostructures, 2023. 18(3): p. 899-913; https://doi.org/10.15251/DJNB.2023.183.899
[45] Zhang, J., et al,. Digest Journal of Nanomaterials and Biostructures, 2023. 18(3): p. 961-974; https://doi.org/10.15251/DJNB.2023.183.961